Therapeutics, Targets, and Chemical Biology

Cancer Research

Monocarboxylate Transporter MCT1 Promotes Tumor Metastasis Independently of Its Activity as a Lactate Transporter

Valéry L. Payen[1], Myriam Y. Hsu[1], Kristin S. Rädecke[1], Elisabeth Wyart[2], Thibaut Vazeille[1], Caroline Bouzin[3], Paolo E. Porporato[1,2], and Pierre Sonveaux[1]

Abstract

Extracellular acidosis resulting from intense metabolic activities in tumors promotes cancer cell migration, invasion, and metastasis. Although host cells die at low extracellular pH, cancer cells resist, as they are well equipped with transporters and enzymes to regulate intracellular pH homeostasis. A low extracellular pH further activates proteolytic enzymes that remodel the extracellular matrix to facilitate cell migration and invasion. Monocarboxylate transporter MCT1 is a passive transporter of lactic acid that has attracted interest as a target for small-molecule drugs to prevent metastasis. In this study, we present evidence of a function for MCT1 in metastasis beyond its role as a transporter of lactic acid. MCT1 activates transcription factor NF-κB to promote cancer cell migration independently of MCT1 transporter activity. Although pharmacologic MCT1 inhibition did not modulate MCT1-dependent cancer cell migration, silencing or genetic deletion of *MCT1 in vivo* inhibited migration, invasion, and spontaneous metastasis. Our findings raise the possibility that pharmacologic inhibitors of MCT1-mediated lactic acid transport may not effectively prevent metastatic dissemination of cancer cells. *Cancer Res; 77(20); 5591–601. ©2017 AACR.*

Introduction

Cancer cells deploy several strategies to survive and proliferate in poorly permissive tumor microenvironments characterized by hypoxia and nutrient deprivation. Among metabolic strategies, hypoxic/glycolytic cancer cells can cooperate with oxidative cancer cells by swapping glycolytic end-product lactic acid against blood-borne glucose (1), and oxidative cancer cells can further obtain lactate by coopting stromal cell metabolism (2, 3). At the core of these metabolic relationships, oxidative cancer cells use lactate as preferential oxidative fuel to glucose, thus sparing glucose for glycolytic cells (1).

Lactate exchanges in cancer are governed by monocarboxylate transporters (MCT) of the *SLC16* gene family that passively convey lactate and protons across the cell membrane (4). MCT1 and MCT4 are the main isoforms expressed by cancer cells (5). With a Km for lactate of 22 to 28 mmol/L and a high turnover rate, hypoxia-inducible MCT4 is adapted for lactic acid export by glycolytic cells (6, 7). Comparatively, MCT1 has a lower 3.5 to 10 mmol/L Km for lactate (4). Considering that the average concentration of lactate is approximately 10 mmol/L in human solid tumors (8) and that oxidative cancer cells consume lactate (1), MCT1 is optimized for lactic acid uptake by these cells. However, as a passive transporter, MCT1 can operate bidirectionally and has also been reported to facilitate lactic acid export from cancer cells (9–12). The directionality of MCT1-driven lactic acid transport indeed depends on the gradient of lactate and protons across membranes.

In growing tumors, functional characterization recently revealed that MCTs are not only gatekeepers of intercellular metabolic cooperation, but also important regulators of angiogenesis. Lactate that enters into oxygenated endothelial cells and oxidative cancer cells *via* MCT1 indeed promotes angiogenesis as it acts as a hypoxia-mimetic that activates transcription factors hypoxia-inducible factor-1 (HIF-1) and nuclear factor-κB (NF-κB), thereby stimulating the production of proangiogenic agents VEGF, bFGF and IL8 (13). Consequently, pharmacologic MCT1 inhibitors have been proposed to simultaneously inhibit lactate exchanges and angiogenesis in tumors with limited side effects (5, 14), making of them particularly good candidate drugs for anticancer treatment. Hence, MCT1 inhibitor AZD3965 is currently tested in phase I/II clinical trials in patients with prostate cancer, gastric cancer, or diffuse large B-cell lymphoma (ClinicalTrials.gov, NCT01791595).

Advanced stage tumors often undergo a metastatic switch, and metastatic dissemination strongly limits curative opportunities. Identifying treatments capable of preventing metastasis is, therefore, an urgent task. At least 3 lines of evidence suggest that lactate and MCTs, especially MCT1, promote tumor metastasis. First, analyses of primary tumor biopsies from patients revealed that high levels of lactate predict the likelihood of tumor metastasis (15–18). Second, MCT1 forms stable heterocomplexes with chaperon protein CD147/basigin (19), and CD147 promotes cancer cell invasion and metastasis (20). Third, we and others recently reported that MCT1 stimulates the migration and invasion of (glucose-starved) cancer cells toward serum or glucose

[1]Pole of Pharmacology, Institut de Recherche Expérimentale et Clinique (IREC), Université catholique de Louvain (UCL), Brussels, Belgium. [2]Department of Molecular Biotechnology and Health Sciences, University of Turin, Turin, Italy. [3]Imaging Platform, Institut de Recherche Expérimentale et Clinique (IREC), Université catholique de Louvain (UCL), Brussels, Belgium.

Note: Supplementary data for this article are available at Cancer Research Online (http://cancerres.aacrjournals.org/).

P.E. Porporato and P. Sonveaux are co-last authors.

Corresponding Author: Pierre Sonveaux, Université catholique de Louvain (UCL), Avenue Emmanuel Mounier 52, Box B1.53.09, 1200 Brussels, Belgium. Phone: 32-2764-5267; Fax: 32-2764-5269; E-mail: pierre.sonveaux@uclouvain.be

doi: 10.1158/0008-5472.CAN-17-0764

(12, 21–23). Gray and colleagues (24) further proposed that MCT1 could facilitate cancer cell migration independently of its transporter activity based on the observation that silencing *MCT1* with an shRNA inhibited the *in vitro* scattering of prostate cancer cells stimulated with EGF or HGF, whereas AZD3965 used at concentrations up to 10 μmol/L did not. In this context, we analyzed the contribution of MCT1 to tumor metastasis. We report that MCT1 activates NF-κB to promote cancer cell migration independently of its transport activity. Consequently, *MCT1* silencing or its genetic deletion inhibited cancer cell migration and invasion *in vitro* and spontaneous tumor metastasis *in vivo*.

Materials and Methods

Cell culture and reagents

Superinvasive SiHa-F3 and mitochondria-deficient SiHa ρ0 cells were generated from wild-type SiHa human cervix adenocarcinoma cells (obtained in 2010 from the ATCC) as in ref. 25. 4T1 mouse mammary carcinoma cells were a kind gift of Fred R. Miller (Karmanos Cancer Institute, Detroit, MI) in 2011. Cells were routinely cultured in DMEM containing 4.5 g/L (25 mmol/L) glucose, GlutaMAX (Gibco), and 10% FBS (Sigma) in a humidified atmosphere at 37°C, 5% CO_2. SiHa ρ0 further received 50 ng/mL of uridine (Sigma) and 1 mmol/L of sodium pyruvate (Gibco). Cells were used from passage 2 to passage 15 after thawing and regularly tested for mycoplasma using the MycoAlert detection Kit (Lonza). MCT1 inhibitors AR-C155858 (Tocris) and AZD3965 (Selleckchem) were dissolved in DMSO. TNFα was from Miltenyi, tetradecanoyl phorbol myristate acetate (TPA) from Sigma-Aldrich, and NF-κB inhibitor BMS-345541 from Tocris. Unless stated otherwise, assays were performed in culture medium.

Transfection and infection

For luciferase expression, 4T1 cells were infected with lentiviruses carrying the luciferase sequence (Addgene 21471) following a previously disclosed protocol (25).

For *MCT1* silencing with siRNAs, SiHa cells were transfected with siCTR (Qiagen; 1027281) or siMCT1 (Qiagen; AAG AGG CUG ACU UUU CCA AAU) as previously described (26) and assayed 48 hours after transfection.

For *MCT1* silencing with shRNAs, cells were infected with lentiviruses as previously described (27). shRNAs targeted human *MCT1* (shMCT1; Thermo Scientific; TRCN0000038339) or mouse *MCT1* (shMCT1a; Thermo Scientific, TRCN0000079545 and shMCT1b; Thermo Scientific, TRCN0000079547). shCTR- and shMCT1-expressing SiHa-F3 cells were further infected with lentiviruses carrying green fluorescent protein (EGFP, Addgene 12252) or red fluorescent tdTomato (Addgene 21374), and the cells were FACS-sorted on an Aria III cell sorter (BD Biosciences). In rescue experiments, mouse 4T1-shMCT1a cells were transfected with human wild-type *MCT1* ($hMCT1^+$) cDNA using pCMV6/Entry-mct1 plasmid (OriGene), and selected with G418 (400 μg/mL).

For *MCT1* deletion, SiHa-CRISPR-MCT1 cells were produced using Sigma LentiCRISPR (Target sequence: GTATAGTCATGATTGTTGGTGG; ref. 27) and selected using puromycin. In rescue experiments, SiHa-CRISPR-MCT1 cells were transfected as in ref. 28 with Cas9-resistant human *MCT1* cDNA (3 conservative point mutations in target sequence: GTATAGTCATGATaGTgGGTGG) that was mutated/inactivated for proton- and lactate-binding sites (38K>R, 302D>R, 306R>D; ref. 29) using pEX-K4-MCT1 plasmid (Eurofins). This mutant transgene was named $hMCT1^-$. pEGFP-c1 (Clontech) was used as a negative and transfection-quality control. Cells were used 96 hours after transfection.

Western blotting

Cells were lysed in RIPA buffer containing inhibitor cocktails of proteases (Sigma) and phosphatases (PhosSTOP; Roche), and Western blotting was performed as previously described (30). Primary antibodies were as follows: rabbit antibodies against MCT1 (Chemicon; #AB3538P), human MCT4 (Chemicon; #AB3316P), mouse MCT4 (Santa Cruz Biotechnology; #sc-50329), p65 (Cell Signaling Technology; #8242), p-Ser536-p65 (Cell Signaling Technology; #3033), IκKα (Cell Signaling Technology; #2682), IκKβ (Cell Signaling Technology; #2370), and mouse antibodies against human CD147 (BD Biosciences; #555961), HSP-90 (BD Biosciences; #610419), and β-actin (Sigma; #A5441). Secondary antibodies were horseradish peroxidase–coupled goat anti-rabbit and anti-mouse (Jackson).

Cell viability and proliferation assay

At day 0, 2,000 SiHa or 4,000 4T1 cells per well were seeded in 96-well plates. Images were daily captured on a SpectraMax miniMax300 imaging cytometer (Molecular Devices) and analyzed with the Softmax Pro software (Molecular Devices). Results were normalized to cell number at day 0.

Cell migration and invasion

Migration was first assayed using a scratch test following a previously disclosed protocol (31). Cells in culture medium containing 0.5 μg/mL of proliferation inhibitor mitomycin C were allowed to migrate for 48 hours in a humidified atmosphere at 37°C, 5% CO_2. To measure scratch closure, images were captured every 4 hours on an Axio Observer.Z1 time lapse microscope (Zeiss). Data were analyzed using ImageJ (NIH).

For transwell assays, cell migration was tested on a multiwell chemotaxis chamber (Neuro Probe) or using transwell inserts (Corning; #353097). Briefly, 50,000 cells in serum-free culture medium were seeded in the upper chamber of each well, and FBS 0.15% was used as a chemoattractant in the lower chamber. Invasion was assayed using transwell inserts (regular Corning #353097 and Fluoroblok Corning #351152) coated with growth factor–reduced and phenol red–free Matrigel (Corning; #356231) diluted 1:10 in PBS. Briefly, 100,000 cells in serum-free culture medium were seeded in the upper chamber of each well, and FBS 5% was used as a chemoattractant in the lower chamber. Cells were allowed to migrate for 16 hours or to invade for 24 hours in a humidified atmosphere at 37°C, 5% CO_2. Migrated/invaded cells were then fixed with methanol. Nonfluorescent cells were stained with a 0.023% crystal violet solution. Images were captured on an AxioVert microscope equipped with an AxioCam-MRc camera (Zeiss), and cells were counted using ImageJ.

Clonogenicity

Clonogenicity was tested on noble agar 0.33% (Sigma). Colonies were allowed to grow for 14 days before staining with a saturated MTT solution (Calbiochem) diluted in PBS. Pictures were taken under a Stemi 2000-C dissection microscope (Zeiss), and colonies were counted using ImageJ.

Metabolic assays

Glucose consumption and lactate release were determined with enzymatic assays on a CMA 600 Microdialysis analyzer (CMA Microdialysis) following manufacturer's instructions. Experimental conditions were as follows: 150,000 SiHa cells/well for 24 hours in 0.5 mL of culture medium and 100,000 4T1 cells/well for 24 hours in 1 mL of culture medium. Results were normalized to total protein content (Bradford).

Intracellular lactate concentration was determined on adherent cells in 96-well plates that were incubated for 30 minutes in 100 μL of culture medium, washed with PBS, and lysed *in situ*. Samples were analyzed using a lactate bioluminescent detection assay kit (kind gift from Promega) according to manufacturer's instructions. Bioluminescence was measured with a GloMax 96 Microplate luminometer (Promega). Data were normalized to cell number.

Oxygen consumption rate (OCR) and extracellular acidification rate (ECAR) were measured on 20,000 cells/well using a Seahorse XF96 analyzer (Agilent) with a combination of XF cell mito stress kit (Agilent) and 2-deoxy-*D*-glucose (2DG; Sigma). Basal mitochondrial OCR is the difference between initial OCR and OCR after inhibition of the electron transport chain by rotenone (0.5 μmol/L) and antimycin A (0.5 μmol/L). Maximal mitochondrial OCR is the difference between OCR after injection of uncoupler FCCP (1 μmol/L) and OCR after injection of rotenone and antimycin A. Glycolytic ECAR is the difference between initial ECAR and ECAR after injection of 2DG (100 mmol/L). All assays were performed in unbuffered serum-free DMEM supplemented with 10 mmol/L *D*-glucose and 2 mmol/L L-glutamine, pH 7.4. Results were normalized to cell number or total protein content (Bradford).

Determination of intracellular and perimembranous pH

Intracellular pH (pHi) was determined on 20,000 cells with 5,6-carboxy-SNARF-1-acetomethylester (SNARF-AM; Molecular Probes) and pH at the outer side of the cell membrane with *N*-(fluorescein-5-thiocarbamoyl)-1,2-dihexadecanoyl-*sn*-glycero-3-phosphoethanolamine (fluorescein-DHPE; Molecular Probes), as previously reported (32). Calibration for pHi was performed on carboxy-SNARF-1–loaded cells treated with potassium/proton ionophore nigericin (2.5 μmol/L) and hyperpotassic solutions at pH values ranging from 6.6 to 8.0. Calibration for extracellular membrane pH was performed with fluorescein-DHPE in solutions at pH 4.9 to 9.2. Fluorescence was measured on a SpectraMax miniMax300 imaging cytometer.

In vivo experiments

All *in vivo* experiments were conducted under approval of the UCL authorities (*Comité d'Ethique Facultaire pour l'Expérimentation Animale*) according to national animal care regulations (authorization #2012/UCL/MD/005).

For spontaneous metastasis assays, 200,000 luciferase-expressing 4T1 cells were subcutaneously injected in the flank of 7-week-old syngeneic BALB/cJRj female mice (Janvier). Primary tumor growth was regularly measured over time with a caliper, and tumor volume was calculated as previously described (33). Primary tumors were surgically resected between days 24 and 31, i.e., when their average diameter reached 10 mm. They were embedded in paraffin, and two 5-μm-thick central sections for each tumor were stained with hematoxylin and eosin (H&E) and immunostained for cleaved caspase-3 (Cell Signaling Technology; #9661) or Ki-67 (Cell Signaling Technology; #12202). All mice were sacrificed at day 38 by cervical dislocation. Ten minutes before sacrifice, mice were i.p. injected with 0.15 mg/g bodyweight of luciferin (PerkinElmer). Five minutes after sacrifice, lungs were inflated with a 15 mg/mL luciferin solution and bathed in the same solution for 5 minutes. Chemiluminescence was acquired on harvested lungs during 4 minutes with a Xenogen IVIS 50 bioluminescence imaging system (PerkinElmer), and quantified with the Living Image software (PerkinElmer). Lungs were further examined under a Stemi 2000-C dissection microscope to count surface metastases. They were then embedded in paraffin, and 5-μm-thick lung sections (2 different plans for each lobe of each animal) were stained with H&E. All slices were scanned with a SCN400 bright field slide scanner (Leica) at ×20 magnification. Quantitative data were obtained with the Tissue IA software (Leica).

Statistical analysis

Except in dot plots that show individual values and group averages, all data show mean ± SEM (error bars are sometimes smaller than symbols). *n* indicates the total number of replicates. Student *t* test, one-way ANOVA with Dunnett or Bonferroni *post hoc* tests, and two-way ANOVA on matched values with Bonferroni *post hoc* test were applied where indicated. $P < 0.05$ was considered to be statistically significant.

Results

MCT1 promotes cancer cell migration and invasion

To address the contribution of MCT1 to cancer metastasis, we used human SiHa cervix squamous carcinoma cells and 4T1 mouse mammary carcinoma cells. Both cell lines express MCT1 (Supplementary Fig. S1A).

In the absence of exogenous lactate except from serum, *MCT1* silencing using siMCT1 or shMCT1 and *MCT1* deletion using a CRISPR-Cas9 strategy (Supplementary Fig. S1A) did not affect SiHa cell count (Supplementary Fig. S1B) but reduced SiHa cell migration (Fig. 1A) and invasion (Fig. 1B) toward serum by about 50% to 80%. A scratch test further revealed that SiHa cell migration was sustainably inhibited by shMCT1 over 48 hours (Supplementary Fig. S1C). Thus, SiHa cell migration and invasion were inhibited upon *MCT1* silencing or deletion. Of note, shMCT1, but not CRISPR-MCT1, was associated with an increase in MCT4 expression (Supplementary Fig. S1A). Expression of CD147/basigin was unchanged. Of further note, providing lactate to SiHa cells barely affected their migratory activity. In transwells, 20 mmol/L of lactate (34) delivered in the upper compartment significantly reduced SiHa migration by about 10%, and lactate did not act as a chemoattractant (Supplementary Fig. S1D).

That MCT1 promotes cancer cell migration was verified in 4T1 cells (see metabolic characterization below). *MCT1* silencing with shMCT1a or shMCT1b (Supplementary Fig. S1A) did not affect clonogenicity (Supplementary Fig. S1E) but reduced 4T1 cell migration by about 65% (Fig. 1C) and invasion by about 40% (Fig. 1D). There was no increase in MCT4 expression upon *MCT1* silencing (Supplementary Fig. S1A).

Suppressing MCT1 expression decreases lactic acid efflux from cancer cells

Because cancer cell metabolism can affect migration, invasion, and metastasis (35), we characterized the metabolic consequences of *MCT1* silencing/deletion in SiHa and 4T1 cells in the same conditions as in migration and invasion assays.

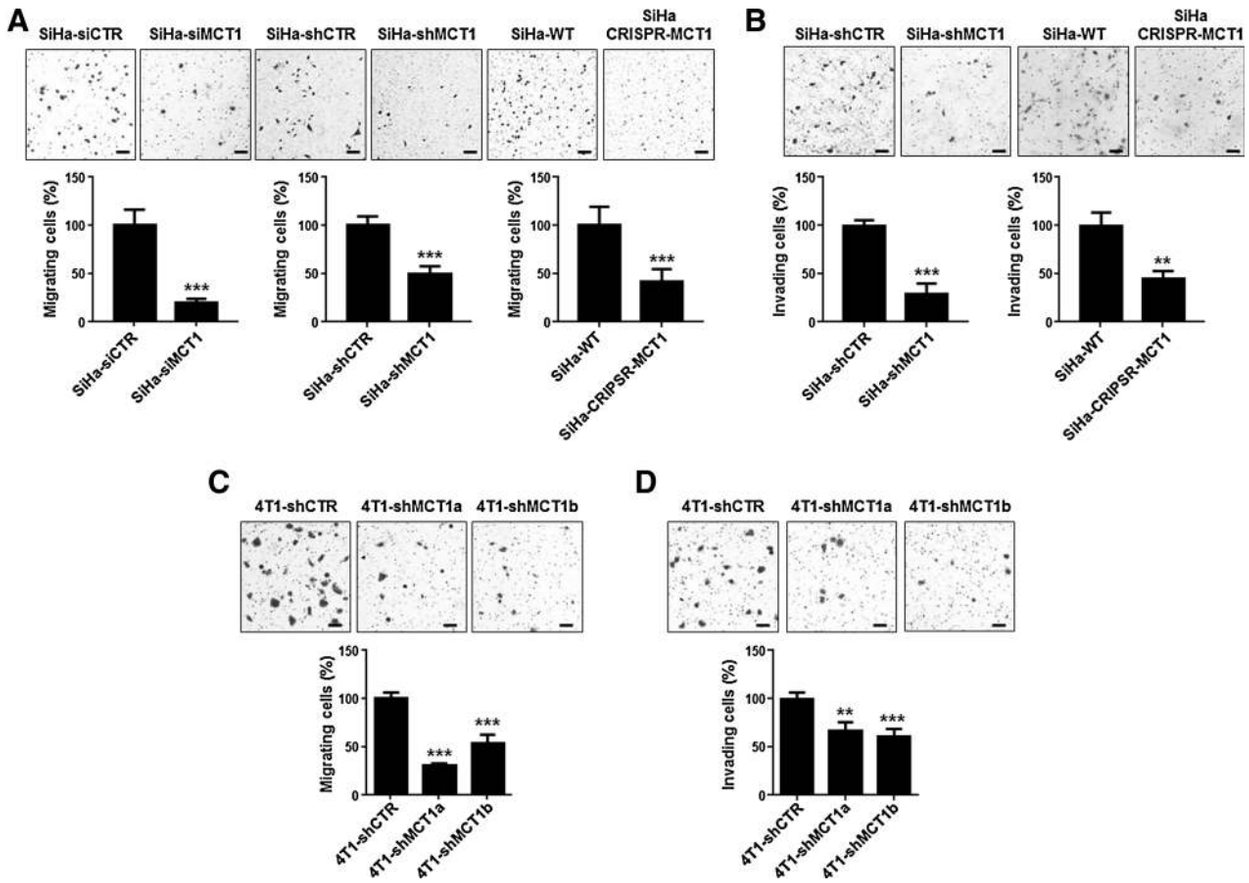

Figure 1.

MCT1 silencing or deletion decreases cancer cell migration and invasion. **A** and **B,** *MCT1* was silenced in SiHa cancer cells using siRNA (SiHa-siMCT1), shRNA (SiHa-shMCT1), or deleted using a CRISPR-Cas9 strategy (SiHa-CRISPR-MCT1). **A,** Comparative migration of SiHa-siCTR versus SiHa-siMCT1 (left; $n = 8$), SiHa-shCTR versus SiHa-shMCT1 (middle; $n = 11$–12), and in SiHa-WT versus SiHa-CRISPR-MCT1 (right; $n = 6$) in a Boyden chamber with 0.15% FBS as chemoattractant. Top plots show representative pictures (bars, 100 μm). **B,** Comparative invasion of SiHa-shCTR versus SiHa-shMCT1 (left; $n = 6$) and in SiHa WT versus SiHa-CRISPR-MCT1 (right; $n = 8$) in a Boyden chamber with 5% FBS as chemoattractant. Top plots show representative pictures (bars, 100 μm). **C** and **D,** *MCT1* was silenced in 4T1 mouse mammary carcinoma cells using two different shRNAs (4T1-shMCT1a and 4T1-shMCT1b). **C,** Cell migration in a Boyden chamber ($n = 16$). Top plots show representative pictures (bars, 100 μm). **D,** Cell invasion in a Boyden chamber ($n = 25$–26). Top plots show representative pictures (bars, 100 μm). **, $P < 0.01$; ***, $P < 0.005$; by Student *t* test (**A** and **B**) or by one-way ANOVA with Dunnett *post hoc* test (**C** and **D**).

In SiHa cells, shMCT1 did not modify glucose consumption (Fig. 2A) but reduced lactate release (Fig. 2B), and lactate accumulated intracellularly (Supplementary Fig. S2A). shMCT1 further decreased the ECAR directly attributable to glycolysis (Fig. 2C), whereas intracellular pH slightly decreased (Supplementary Fig. S2B). pH at the outer side of the cell membrane was less acidic (Supplementary Fig. S2C). Similarly, deleting *MCT1* using CRISPR-Cas9 resulted in decreased lactate release (Fig. 2B) and decreased glycolytic ECAR (Fig. 2C) with unchanged glucose consumption (Fig. 2A). Lactate accumulated intracellularly (Supplementary Fig. S2A). Thus, inhibiting MCT1 expression decreased the glycolytic efficiency of SiHa cells. Oxidative activity was measured on a Seahorse XF96 oximeter. Compared with shCTR, shMCT1 did not modify the basal OCR of SiHa cells or their maximal respiratory capacity (Fig. 2D–F). In contrast, both parameters increased in SiHa-CRISPR-MCT1 compared with wild-type SiHa cells (Fig. 2D–F).

Metabolic characterization was also performed for 4T1 cells. Compared with shCTR, shMCT1a and shMCT1b decreased 4T1 glucose consumption (Fig. 2G) and lactate release (Fig. 2H), which was associated to a decreased glycolytic ECAR (Fig. 2I). Basal and maximal OCR increased (Fig. 2J), especially with shMCT1b that was more efficient than shMCT1a to repress MCT1 protein expression in these cells (Supplementary Fig. S1A).

The transporter activity of MCT1 does not participate in MCT1-dependent cancer cell migration and invasion

An acidic environment promotes cancer cell migration, invasion, and metastasis (35). Because as a passive transporter MCT1 can transport lactic acid bidirectionally, we investigated whether MCT1 activity is involved in the prometastatic phenotype. Inhibition of MCT1 with increasing doses of AR-C155858 (27) or 10 μmol/L of AZD3965 (24) did not significantly modify glucose consumption (Fig. 3A) but reduced lactate release (Fig. 3B) by SiHa cells, and lactate accumulated intracellularly (Supplementary Fig. S3A). AR-C155858 also reduced proton export by the cells (Fig. 3C) and promoted intracellular acidification (Supplementary Fig. S3B). At 10 μmol/L, it did not affect the OCR of the

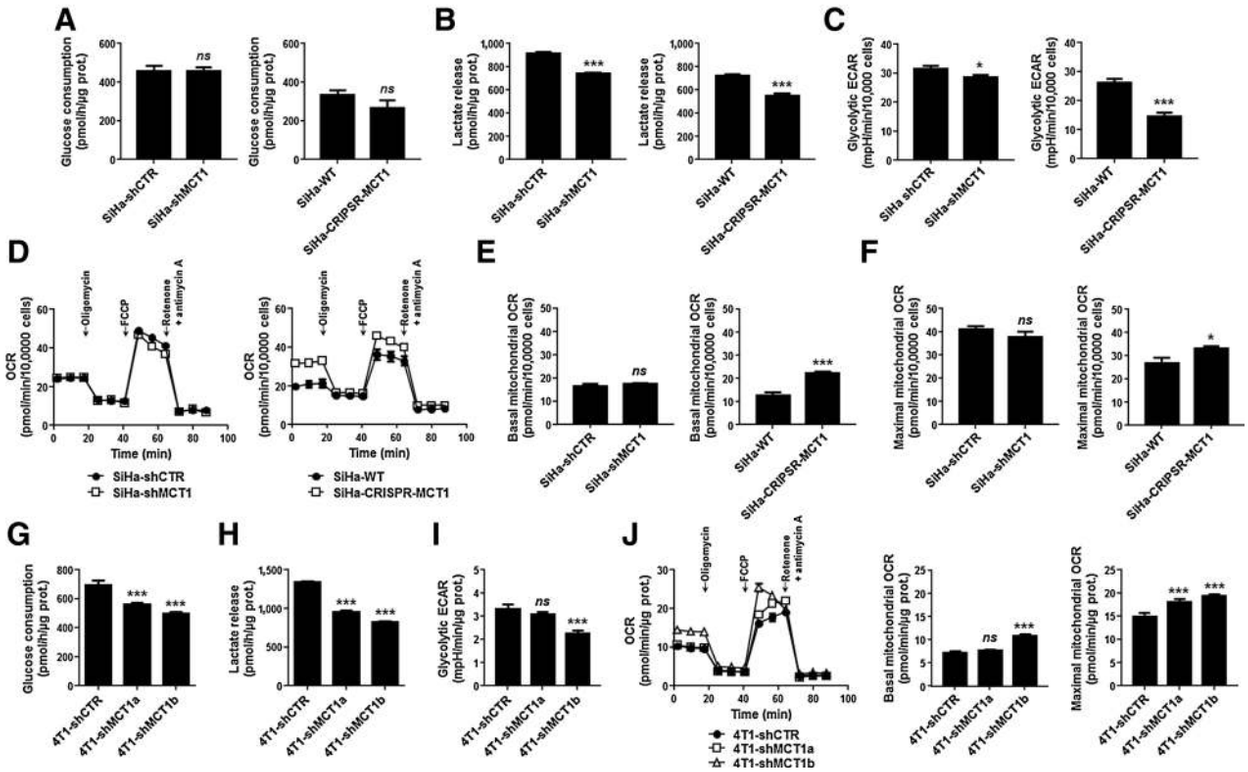

Figure 2.

MCT1 silencing or deletion decreases lactic acid efflux from SiHa and 4T1 cells. **A–F,** *MCT1* was silenced in SiHa cancer cells using shRNA (SiHa-shMCT1) or deleted using CRISPR-Cas9 (SiHa-CRISPR-MCT1). **A,** Glucose consumption by SiHa-shCTR versus SiHa-shMCT1 (left; $n = 6$) and in SiHa WT versus SiHa-CRISPR-MCT1 (right; $n = 5$–6). **B,** Lactate release by SiHa-shCTR versus SiHa-shMCT1 (left; $n = 6$) and in SiHa WT versus SiHa-CRISPR-MCT1 (right; $n = 5$–6). **C,** Glycolytic ECAR measured with a Seahorse analyzer in SiHa-shCTR versus SiHa-shMCT1 (left; $n = 15$) and in SiHa WT versus SiHa-CRISPR-MCT1 (right; $n = 7$–8). **D,** OCR measured with a Seahorse analyzer in SiHa-shCTR versus SiHa-shMCT1 (left; $n = 13$–15) and in SiHa WT versus SiHa-CRISPR-MCT1 (right; $n = 7$–8). **E,** Basal mitochondrial OCR calculated from **D**. **F,** Maximal mitochondrial OCR calculated from **D**. **G–J,** *MCT1* was silenced using two different shRNAs in 4T1-shMCT1a and 4T1-shMCT1b cells. **G,** Glucose consumption ($n = 3$). **H,** Lactate release ($n = 3$). **I,** Glycolytic ECAR ($n = 7$). **J,** OCR, basal mitochondrial OCR and maximal mitochondrial OCR ($n = 7$). ns, nonsignificant, $P > 0.05$; *, $P < 0.05$; ***, $P < 0.005$; by Student *t* test (**A–F**) or one-way ANOVA with Dunnett *post hoc* test (**G–J**).

cells (Supplementary Fig. S3C) or their number (Supplementary Fig. S3D). However, despite the striking similarity of the metabolic effects seen with *MCT1* suppression and its inhibition, AR-C155858 did not inhibit SiHa cell migration (Fig. 3D) or invasion (Fig. 3E). AZD3965 (10 µmol/L) did not impair SiHa cell migration (Fig. 3D). Of note, we verified that neither AR-C155858 nor AZD3965 altered MCT1, MCT4, and CD147 expression in the cells (Supplementary Fig. S3E).

In 4T1 cells, AR-C155858 was used at a 10 nmol/L concentration that did not affect cell number (Supplementary Fig. S3F) but efficiently decreased glucose consumption (Fig. 3F) and lactic acid release (Fig. 3G and Supplementary Fig. S3G). AR-C155858 did not affect 4T1 cell migration (Fig. 3H) or invasion (Fig. 3I). MCT1 was also re-expressed in 4T1-shMCT1a cells, and we opted for a human sequence resistant to the anti-mouse shRNA ($hMCT1^+$), which restored 4T1 cell migration (Fig. 3J).

To demonstrate that MCT1 promotes cancer cell migration independently of its transporter activity, we generated a Cas9-resistant and transport-inactive (38K>R, 302D>R, 306R>D; ref. 29) version of the transporter ($hMCT1^-$). Expression of $hMCT1^-$ in SiHa-CRISPR-MCT1 cells restored migration (Fig. 3K). EGFP was used in control experiments, evidencing that about 50% of the cells were efficiently transfected (Supplementary Fig. S3H).

Highly invasive cancer cells have a high MCT1 expression that promotes their migration and invasion

To further analyze the relationship between MCT1 expression and the prometastatic phenotype, we used SiHa-F3 and SiHa-ρ0 cells, which have been reported to be more migratory and invasive than SiHa-WT (25).

SiHa-F3 had increased MCT1 expression compared with SiHa-WT, whereas MCT4 expression was decreased and CD147 expression was unmodified (Fig. 4A). Compared with SiHa-WT, SiHa-F3 cells had increased glucose consumption (Supplementary Fig. S4A) and lactate release (Supplementary Fig. S4B), increased glycolytic ECAR (Supplementary Fig. S4C), and increased basal OCR (Supplementary Fig. S4D). They were more migratory than SiHa-WT cells (Fig. 4B and Supplementary Fig. S4E). Conversely, silencing *MCT1* with shMCT1 in SiHa-F3 cells (Fig. 4A) decreased lactate release (Supplementary Fig. S4B) and increased cell respiration (Supplementary Fig. S4D). shMCT1, but not AR-C155858, significantly decreased SiHa-F3 cell migration and invasion (Fig. 4B and C; Supplementary Fig. S4E).

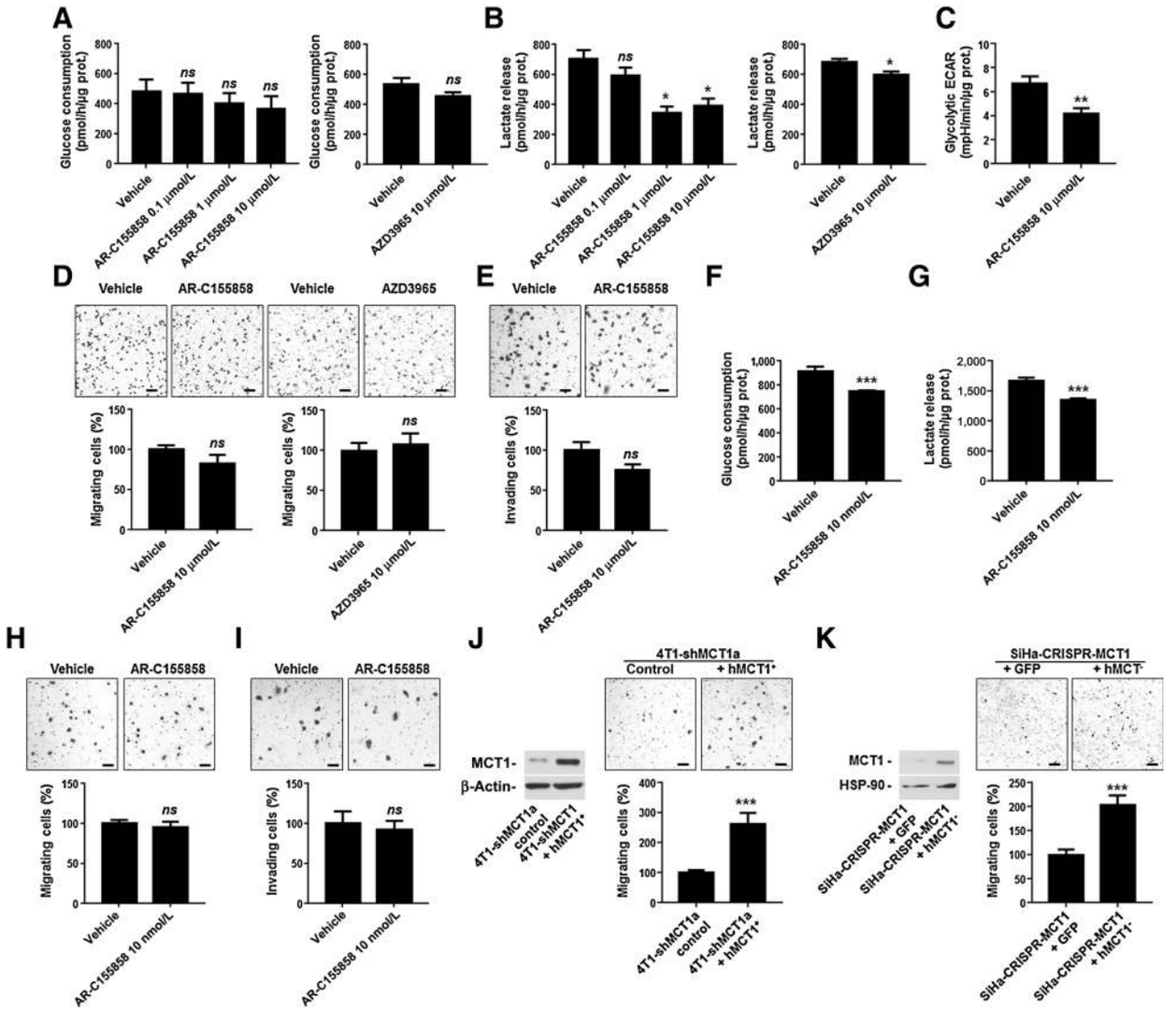

Figure 3.

Pharmacologic MCT1 inhibition decreases lactic acid efflux but does affect cancer cell migration and invasion. **A–I,** MCT1 activity was inhibited in cancer cells by AR-C155858 or AZD3965. Vehicle was 0.1% DMSO. **A,** Glucose consumption by SiHa-WT cells treated with AR-C155858 (left; $n = 8$–9) or AZD3965 (right; $n = 5$–6) versus vehicle. **B,** Lactate release by SiHa-WT cells treated with AR-C155858 (left; $n = 8$–9) or AZD3965 (right; $n = 5$–6) versus vehicle. **C,** Glycolytic ECAR of SiHa-WT cells ($n = 6$). **D,** SiHa-WT cell migration when treated with AR-C155858 (left; $n = 15$) or AZD3965 (right; $n = 12$) versus vehicle in a Boyden Chamber. Top plots show representative pictures (bars, 100 µm). **E,** SiHa WT cell invasion in a Boyden Chamber ($n = 10$). Top plots show representative pictures (bars, 100 µm). **F,** Glucose consumption of 4T1 cells ($n = 6$). **G,** Lactate release by 4T1 cells ($n = 6$). **H,** 4T1 cell migration ($n = 12$). Top plots show representative pictures (bars, 100 µm). **I,** 4T1 cell invasion ($n = 12$). Top plots show representative pictures (bars, 100 µm). **J,** Migration of 4T1 cells silenced for *MCT1* (shMCT1a) and expressing or not wild-type human MCT1 (hMCT1$^+$; $n = 8$). Western blots show MCT1 and β-actin expression ($n = 3$). Top plots show representative pictures (bars, 100 µm). **K,** Migration of SiHa cells deleted for *MCT1* using CRISPR-Cas9 (SiHa-CRISPR-MCT1) and expressing or not mutated/inactive human MCT1 (hMCT1$^-$; $n = 12$). Western blots show MCT1 and HSP-90 expression ($n = 2$). Top plots show representative pictures (bars, 100 µm). ns, nonsignificant, $P > 0.05$; *, $P < 0.05$; **, $P < 0.01$; ***, $P < 0.005$; by one-way ANOVA with Dunnett *post hoc* test (**A–B**, left) or by Student *t* test (**A–B**, right; **C–K**).

Similarly, SiHa-ρ0 cells expressed more MCT1 compared with parental cells (Fig. 4D). Their *in vitro* migration and invasion was almost fully inhibited upon *MCT1* silencing (Fig. 4E).

MCT1 expression, but not its transport activity, triggers NF-κB in cancer cells

We next sought to identify a mechanism through which MCT1 expression could control cancer cell migration independently of its activity as a transporter. Based on a previous report by Zhao and colleagues (36), we focused on transcription factor NF-κB. Compared with SiHa-WT, SiHa-F3 and SiHa-ρ0 cells had a higher phospho-Ser536-p65/total p65 ratio (Supplementary Fig. S5A). Conversely, both SiHa-shMCT1 and SiHa-CRISPR-MCT1 had a decreased phospho-Ser536-p65/total p65 ratio than control cells (Fig. 5A). Upstream in the NF-κB pathway, *MCT1* deletion decreased IκKα but not IκKβ expression (Fig. 5B). Similarly, the phospho-Ser536-p65/total p65 ratio was decreased in 4T1 cells expressing shMCT1a or shMCT1b (Fig. 5C) and restored when

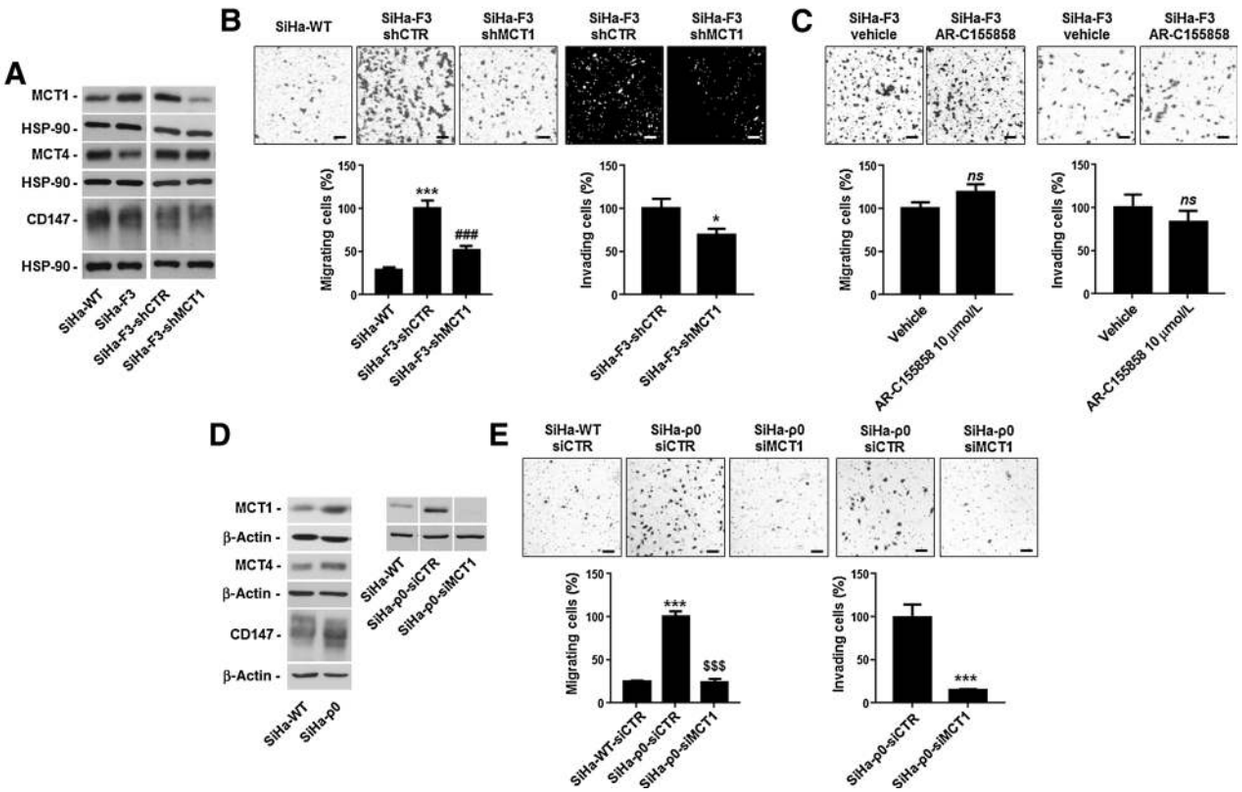

Figure 4.

Superinvasive SiHa-F3 and SiHa-ρ0 cells have high MCT1 expression that promotes migration and invasion. **A–F,** Where indicated, *MCT1* was silenced using siMCT1 or shMCT1. **A,** Representative Western blots of MCT1, MCT4, CD147, and HSP-90 expression. **B,** SiHa-F3 migration (left; $n = 4$) and invasion (right; $n = 17$–18) in Boyden chambers. Top plots show representative pictures (bars, 100 µm). **C,** SiHa-F3 migration (left; $n = 10$) and invasion (right; $n = 12$) upon treatment with 10 µmol/L of AR-C155858 or vehicle. Top plots show representative pictures (bars, 100 µm). **D,** Representative Western blots of MCT1, MCT4, CD147, and β-actin expression. **E,** SiHa-ρ0 migration (left; $n = 4$) and invasion (right; $n = 8$). Top plots show representative pictures (bars, 100 µm). ns, nonsignificant, $P > 0.05$; *, $P < 0.05$; ***, $P < 0.005$ versus control; ###, $P < 0.005$ versus SiHa-F3-shCTR; $$$, $P < 0.005$ versus SiHa-ρ0-siCTR; by one-way ANOVA with Dunnett *post hoc* test (**B**, left; **E**, left) or Student *t* test (**B**, right; **C** and **E**, right).

4T1-shMCT1 cells expressed hMCT1$^+$ (Supplementary Fig. S5B). Of note, expression of mutated/inactivated hMCT1$^-$ in SiHa-CRISPR-MCT1 cells also increased p65 Ser536-phosphorylation (Supplementary Fig. S5C), but cellular stress induced by the transfection procedure had a confounding effect.

Because changes in MCT1 expression but not its pharmacologic inhibition by AR-C155858 or AZD3965 (Supplementary Fig. S5D) influenced p65 phosphorylation, we tested whether NF-κB activation was sufficient to resume MCT1-deficent cell migration. NF-κB activation by TNFα or TPA (Supplementary Fig. S5E) restored SiHa-CRISPR-MCT1 cell migration (Fig. 5D), and this effect was fully blocked by BMS-345541, a highly specific NF-κB inhibitor (Supplementary Fig. S5E; ref. 37). NF-κB inhibition and *MCT1* deletion had no additive antimigratory effects (Fig. 5E), which, together with the above data, indicated that NF-κB acts downstream of MCT1 to control cancer cell migration.

MCT1 silencing inhibits spontaneous 4T1 breast cancer metastasis to the lungs

SiHa cells are only weakly metastatic in SCID mice (38). To evaluate the contribution of MCT1 expression to metastasis, we therefore used the 4T1 model where primary tumors spontaneously metastasize to the lungs of immunocompetent syngeneic mice (39). Luciferase-expressing 4T1-shCTR, 4T1-shMCT1a, and 4T1-shMCT1b cells generated subcutaneous primary tumors with similar growth rates (Supplementary Fig. S6A), necrotic cores, and apoptotic and proliferative fractions (Supplementary Fig. S6B). However, *MCT1* silencing strongly decreased lung metastasis detected by *ex vivo* bioluminescence (Fig. 6A) and direct counts (Fig. 6B). These data were confirmed by histologic analysis showing fewer (Fig. 6C, left) and smaller (Fig. 6C, right) metastases per total lung area in 4T1-shMCT1a and 4T1-MCT1b compared with 4T1-shCTR tumor-bearing mice.

Discussion

This study aimed to clarify the contribution of MCT1 to cancer metastasis. We report that MCT1 promotes cancer cell migration and invasion independently of its activity as a transporter. Consequently, *MCT1* silencing or deletion, but not its pharmacologic inhibition, repressed these phenotypes. Silencing *MCT1* further inhibited spontaneous metastatic dissemination in mice.

Since its identification as a transporter of lactic acid in cancer cells in 1994 (40) and in tumors in 2001 (41), MCT1 expression has been reported in a wide variety of human cancers, including head and neck, breast, lung, stomach, colon, bladder, prostate and

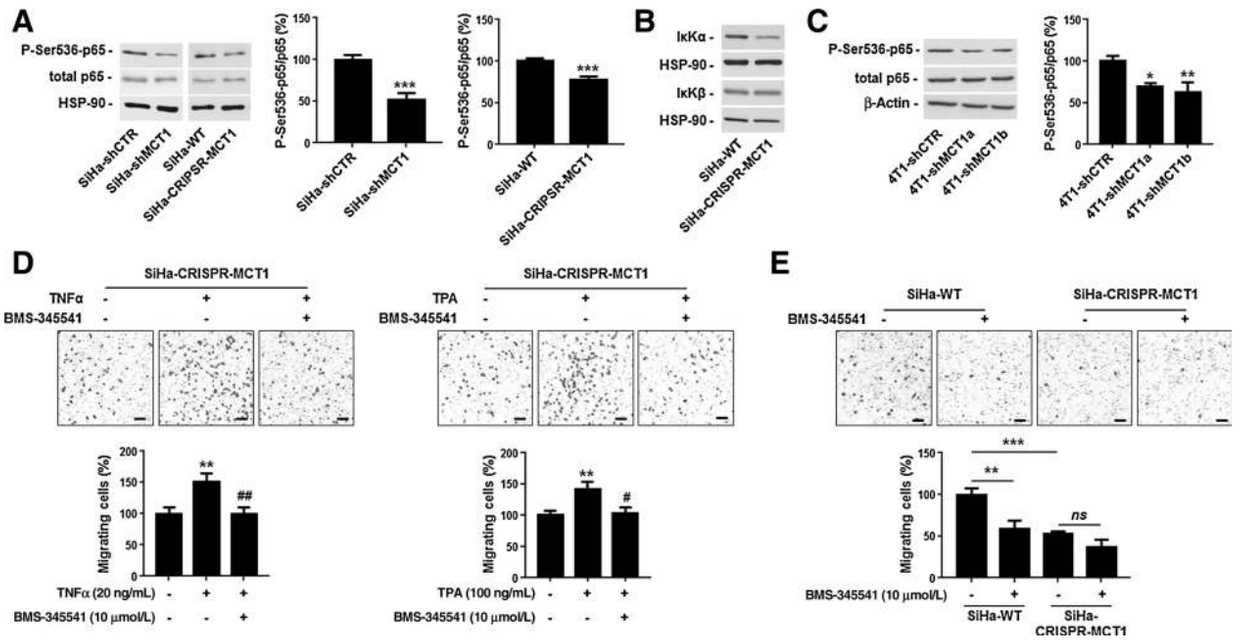

Figure 5.

NF-κB controls MCT1-dependent cancer cell migration. **A,** Comparison of phospho-Ser536-p65, total p65, and HSP-90 protein expression in SiHa-shCTR versus SiHa-shMCT1 ($n = 6$) and SiHa-WT versus SiHa-CRISPR-MCT1 ($n = 9$). **B,** Representative blots of IκKα, IκKβ, and HSP-90 in SiHa-WT and SiHa-CRISPR-MCT1 cells ($n = 6$–12). **C,** Comparison of phospho-Ser536-p65, total p65, and β-actin protein expression in 4T1-shCTR versus 4T1-shMCT1a and 4T1-shMCT1b cells ($n = 9$). **D,** Migration in a Boyden chamber of SiHa-CRISPR-MCT1 cells pretreated for 2 hours ± TNFα (left; $n = 12$) or TPA (right; $n = 15$) with or without NF-κB inhibitor BMS-345541. Top plots show representative pictures (bars, 100 μm). **E,** Migration in a Boyden chamber of SiHa-WT and SiHa-CRISPR-MCT1 cells pretreated for 24 hours and treated during the assay ± BMS-345541 ($n = 8$). Top plots show representative pictures (bars, 100 μm). ns, nonsignificant, $P > 0.05$; *, $P < 0.05$; **, $P < 0.01$; ***, $P < 0.005$ versus first column or as indicated; #, $P < 0.05$; ##, $P < 0.01$ versus second column; by Student *t* test (**A**) or one-way ANOVA with Dunnett (**C–D**) or Bonferroni (**E**) *post hoc* test.

cervix cancers, as well as gliomas [(see references in (5)]. Its transporter activity has been positively linked to the metabolic capability of cancer cells to switch substrates depending on their local bioavailability (5) and to tumor angiogenesis (13). However, to our knowledge and despite converging clues (12, 21–24, 36), there was no experimental demonstration that MCT1 contributes to tumor metastasis *in vivo*. The closest related study is probably that of Zhao and colleagues (36) who claimed that downregulation of MCT1 expression inhibits tumor metastasis, but these authors did not perform any *in vivo* experiments. Our demonstration that MCT1 promotes spontaneous tumor metastasis in immunocompetent mice thus confirms these previous hypothetical clues. Together with our precedent observations, it reveals that MCT1 facilitates three main strategies displayed by cancer cells in harsh microenvironmental conditions: to adapt to the environment (metabolic plasticity), to modify the environment (angiogenesis), and to leave the environment (migration, invasion, and metastasis). Thus, high MCT1 expression facilitates cancer cell migration, invasion, and metastasis. This characteristic is shared by different cancer cell types, including superinvasive SiHa-F3 and SiHa-ρ0 cervix adenocarcinoma cells that depend on high MCT1 expression for migration and invasion (this study) and clinical non-small cell lung carcinomas (42) where metastatic lesions express higher levels of MCT1 than primary tumors. The latter observation further indicates that MCT1 could contribute to the growth of established metastases.

As a passive transporter, MCT1 can operate bidirectionally, which explains why it facilitated lactic acid export from SiHa and 4T1 cells in our experimental conditions. Accordingly, MCT1-deficient cells had a reduced capacity to acidify culture medium in general and the outer side of the cell membrane in particular. Generally, extracellular acidification triggers cell invasion by promoting protease activity and altering cellular adhesion (35, 43), but MCT1 turned out not to be an essential contributor to pH-dependent invasion. Indeed, although MCT1 inhibitors AR-C155858 and AZD3965 effectively reduced lactic acid release by the cells, they did not inhibit migration and invasion even when used at doses higher than what can be safely achieved *in vivo*. This observation can be related to the presence of several other sources of acidity, including CO_2, as notably evidenced by experiments that showed that glycolysis-deficient cancer cells that produce negligible amounts of lactic acid are as effective as glycolysis-competent cells to lower extracellular pH down to 6.7 (44). Thus, in agreement with Gray and colleagues (24) but not with Izumi and colleagues (22) who used nonselective MCT inhibitors, we report that MCT1 promotes cancer cell migration and invasion independently of its transporter activity. In support of this conclusion, expression of a transport-inactivated version of MCT1 lacking proton- and lactate-binding sites in *MCT1*-deleted cancer cells rescued migration.

Mechanistically, based on previous observations (36), we confirmed that NF-κB is a downstream effector of MCT1 for cancer cell migration. Indeed, *MCT1* deletion reduced the expression of IκKα (a catalytically active constituent of the IκB kinase complex that normally triggers NF-κB activation) and reduced NF-κB activity and cell migration, and *MCT1* deletion and NF-κB inhibition had

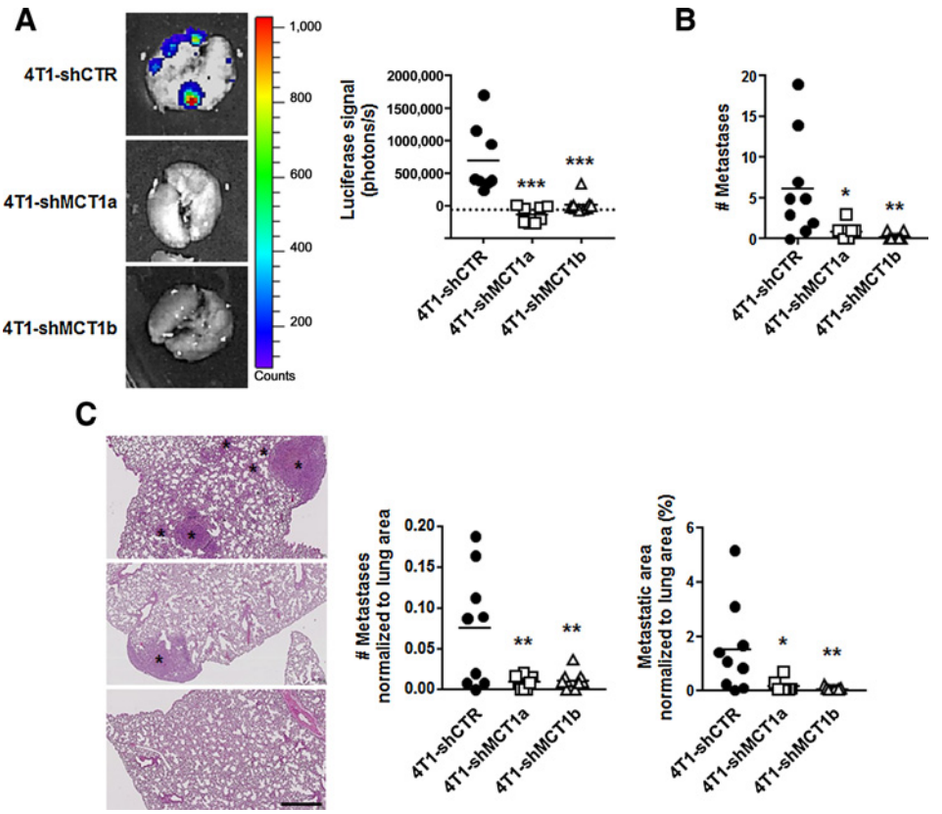

Figure 6.

MCT1 silencing decreases spontaneous 4T1 metastasis. Spontaneous lung metastasis assay using luciferase-expressing 4T1-shCTR, 4T1-shMCT1a, and 4T1-shMCT1b cancer cells that were implanted subcutaneously to form primary tumors in immunocompetent syngeneic mice. Lungs were analyzed 38 days after primary tumor implantation. **A,** Representative pictures and quantification of the luciferase signal in mouse lungs ($n = 8$–9). **B,** Quantification of the number of surface metastases in mouse lungs ($n = 8$–9). **C,** Representative micrographs of H&E-stained lung sections where metastases are indicated with an asterisk and quantification of the number of metastases (left) and metastatic area (right) normalized to lung area ($n = 8$–9). *, $P < 0.05$; **, $P < 0.01$; ***, $P < 0.005$; by one-way ANOVA with Dunnett *post hoc* test (**A–C**).

no additive effects on inhibition of cancer cell migration. Conversely, NF-κB activation restored the migration of *MCT1*-deficient cells, which was achieved either with pharmacologic NF-κB activators or through MCT1 re-expression in deficient cells. Beyond its role as a transporter, MCT1 physically interacts with proteins, notably carbonic anhydrase II (CAII; ref. 45), hyaluronan receptor CD44 (46), and CD147 (19). While cytosolic CAII regulates MCT1 transporter activity (47) and CD44 is a stem cell marker, transmembrane glycoprotein CD147, also known as extracellular matrix metalloproteinase inducer (EMMPRIN), is well known to promote tumor metastasis (48). Interestingly, through a yet unknown mechanism, CD147 has been reported to activate NF-κB in cardiomyocytes (49) and in fibroblasts (50). Because interaction mutually stabilizes both proteins at the cell membrane, it would have been tempting to propose that MCT1-CD147 complexes could promote cancer cell migration and invasion through CD147-dependent NF-κB activation. However, CD147 expression was not altered in our MCT1-defective cell models, most probably because CD147 interacts with other proteins at the cell membrane, notably MCT4 (19). Thus, how MCT1 expression represses IκKα expression and activates NF-κB in cancer cells independently of lactate fluxes remains an open question. Hypotheses that merit to be addressed relate to the turnover rate of CD147 in *MCT1*-deficient cells, as the extracellular domain of CD147 has been proposed to control IκB kinase expression, of which IκKα is a constituent (50), and the possibility that MCT1 itself would initiate intracellular signaling through yet unknown protein–protein interaction(s). MCT1 could also further trigger NF-κB–independent pathways to promote cancer cell migration.

Conclusively, MCT1 activates NF-κB independently of its transporter activity, which promotes cancer cell migration, invasion, and metastasis. We therefore believe that MCT1 inhibitors do not have the potential to achieve a clinical prevention of tumor metastasis, which of course does not affect their therapeutic interest as antimetabolic and antiangiogenic drugs in established (primary and secondary) tumors.

Disclosure of Potential Conflicts of Interest

No potential conflicts of interest were disclosed.

Authors' Contributions

Conception and design: V.L. Payen, C. Bouzin, P.E. Porporato, P. Sonveaux
Development of methodology: V.L. Payen, E. Wyart, P.E. Porporato, P. Sonveaux
Acquisition of data (provided animals, acquired and managed patients, provided facilities, etc.): V.L. Payen, M.Y. Hsu, K.S. Rädecke, T. Vazeille
Analysis and interpretation of data (e.g., statistical analysis, biostatistics, computational analysis): V.L. Payen, M.Y. Hsu, K.S. Rädecke, T. Vazeille, P. Sonveaux
Writing, review, and/or revision of the manuscript: V.L. Payen, M.Y. Hsu, K.S. Rädecke, E. Wyart, T. Vazeille, C. Bouzin, P.E. Porporato, P. Sonveaux
Administrative, technical, or material support (i.e., reporting or organizing data, constructing databases): P. Sonveaux
Study supervision: P.E. Porporato, P. Sonveaux
Other (obtaining all financial support for the study): P. Sonveaux

Acknowledgments

The authors thank Fred R. Miller (B.A. Karmanos Cancer Institute, Detroit, MI) for the kind gift of the 4T1 cells; Marylène Focant (Promega) for the kind gift of lactate bioluminescent detection assay kits; Vincent F. Van Hée, Emilia Turco, Jean-François Toubeau, Marie-Christine Many, and Lucie Brisson for scientific

input and discussions; and Morgane Tardy, Chantal Fregimilicka, Michèle De Beukelaer, Catherine Lombard, and Joachim Ravau for excellent technical support.

Grant Support

This work was supported by a Starting Grant from the European Research Council (ERC No. 243188 TUMETABO to P. Sonveaux), Interuniversity Attraction Pole (IAP) grant #UP7-03 from the Belgian Science Policy Office (Belspo; to P. Sonveaux), an Action de Recherche Concertée from the Communauté Française de Belgique (ARC 14/19-058 to P. Sonveaux), the Belgian Fonds National de la Recherche Scientifique (F.R.S.-FNRS; to P. Sonveaux), the Belgian Fondation contre le Cancer (Fundamental Research Grant #F86 to P. Sonveaux), the Télévie (to P. Sonveaux), the Fonds Joseph Maisin (to P.E. Porporato and P. Sonveaux), and the Louvain Foundation (to P. Sonveaux). P. Sonveaux is a Senior Research Associate, and V.L. Payen is a PhD Fellow of the F.R.S.-FNRS.

The costs of publication of this article were defrayed in part by the payment of page charges. This article must therefore be hereby marked *advertisement* in accordance with 18 U.S.C. Section 1734 solely to indicate this fact.

Received March 15, 2017; revised July 18, 2017; accepted August 14, 2017; published OnlineFirst August 21, 2017.

References

1. Sonveaux P, Vegran F, Schroeder T, Wergin MC, Verrax J, Rabbani ZN, et al. Targeting lactate-fueled respiration selectively kills hypoxic tumor cells in mice. J Clin Invest 2008;118:3930–42.
2. Pavlides S, Whitaker-Menezes D, Castello-Cros R, Flomenberg N, Witkiewicz AK, Frank PG, et al. The reverse Warburg effect: aerobic glycolysis in cancer associated fibroblasts and the tumor stroma. Cell Cycle 2009; 8:3984–4001.
3. Fiaschi T, Marini A, Giannoni E, Taddei ML, Gandellini P, De Donatis A, et al. Reciprocal metabolic reprogramming through lactate shuttle coordinately influences tumor-stroma interplay. Cancer Res 2012; 72:5130–40.
4. Halestrap AP, Wilson MC. The monocarboxylate transporter family–role and regulation. IUBMB Life 2012;64:109–19.
5. Perez-Escuredo J, Van Hee VF, Sboarina M, Falces J, Payen VL, Pellerin L, et al. Monocarboxylate transporters in the brain and in cancer. BBA Mol Cell Res 2016;1863:2481–97.
6. Dimmer KS, Friedrich B, Lang F, Deitmer JW, Broer S. The low-affinity monocarboxylate transporter MCT4 is adapted to the export of lactate in highly glycolytic cells. Biochem J 2000;350(Pt 1):219–27.
7. Ullah MS, Davies AJ, Halestrap AP. The plasma membrane lactate transporter MCT4, but not MCT1, is up-regulated by hypoxia through a HIF-1alpha-dependent mechanism. J Biol Chem 2006;281:9030–7.
8. Walenta S, Schroeder T, Mueller-Klieser W. Lactate in solid malignant tumors: potential basis of a metabolic classification in clinical oncology. Curr Med Chem 2004;11:2195–204.
9. Le Floch R, Chiche J, Marchiq I, Naiken T, Ilk K, Murray CM, et al. CD147 subunit of lactate/H+ symporters MCT1 and hypoxia-inducible MCT4 is critical for energetics and growth of glycolytic tumors. Proc Natl Acad Sci U S A 2011;108:16663–8.
10. Polanski R, Hodgkinson CL, Fusi A, Nonaka D, Priest L, Kelly P, et al. Activity of the monocarboxylate transporter 1 inhibitor AZD3965 in small cell lung cancer. Clin Cancer Res 2014;20:926–37.
11. Morais-Santos F, Granja S, Miranda-Goncalves V, Moreira AH, Queiros S, Vilaca JL, et al. Targeting lactate transport suppresses in vivo breast tumour growth. Oncotarget 2015;6:19177–89.
12. Miranda-Goncalves V, Granja S, Martinho O, Honavar M, Pojo M, Costa BM, et al. Hypoxia-mediated upregulation of MCT1 expression supports the glycolytic phenotype of glioblastomas. Oncotarget 2016;7:46335–53.
13. Payen VL, Brisson L, Dewhirst MW, Sonveaux P. Common responses of tumors and wounds to hypoxia. Cancer J 2015;21:75–87.
14. Dhup S, Dadhich RK, Porporato PE, Sonveaux P. Multiple biological activities of lactic acid in cancer: influences on tumor growth, angiogenesis and metastasis. Curr Pharm Des 2012;18:1319–30.
15. Walenta S, Salameh A, Lyng H, Evensen JF, Mitze M, Rofstad EK, et al. Correlation of high lactate levels in head and neck tumors with incidence of metastasis. Am J Pathol 1997;150:409–15.
16. Brizel DM, Schroeder T, Scher RL, Walenta S, Clough RW, Dewhirst MW, et al. Elevated tumor lactate concentrations predict for an increased risk of metastases in head-and-neck cancer. Int J Radiat Oncol Biol Phys 2001;51:349–53.
17. Schwickert G, Walenta S, Sundfor K, Rofstad EK, Mueller-Klieser W. Correlation of high lactate levels in human cervical cancer with incidence of metastasis. Cancer Res 1995;55:4757–9.
18. Walenta S, Wetterling M, Lehrke M, Schwickert G, Sundfor K, Rofstad EK, et al. High lactate levels predict likelihood of metastases, tumor recurrence, and restricted patient survival in human cervical cancers. Cancer Res 2000;60:916–21.
19. Wilson MC, Meredith D, Fox JE, Manoharan C, Davies AJ, Halestrap AP. Basigin (CD147) is the target for organomercurial inhibition of monocarboxylate transporter isoforms 1 and 4: the ancillary protein for the insensitive MCT2 is EMBIGIN (gp70). J Biol Chem 2005;280:27213–21.
20. Pan Y, He B, Song G, Bao Q, Tang Z, Tian F, et al. CD147 silencing via RNA interference reduces tumor cell invasion, metastasis and increases chemosensitivity in pancreatic cancer cells. Oncol Rep 2012;27:2003–9.
21. De Saedeleer CJ, Porporato PE, Copetti T, Perez-Escuredo J, Payen VL, Brisson L, et al. Glucose deprivation increases monocarboxylate transporter 1 (MCT1) expression and MCT1-dependent tumor cell migration. Oncogene 2014;33:4060–8.
22. Izumi H, Takahashi M, Uramoto H, Nakayama Y, Oyama T, Wang KY, et al. Monocarboxylate transporters 1 and 4 are involved in the invasion activity of human lung cancer cells. Cancer Sci 2011;102:1007–13.
23. Kong SC, Nohr-Nielsen A, Zeeberg K, Reshkin SJ, Hoffmann EK, Novak I, et al. Monocarboxylate transporters MCT1 and MCT4 regulate migration and invasion of pancreatic ductal adenocarcinoma cells. Pancreas 2016; 45:1036–47.
24. Gray AL, Coleman DT, Shi R, Cardelli JA. Monocarboxylate transporter 1 contributes to growth factor-induced tumor cell migration independent of transporter activity. Oncotarget 2016;7:32695–706.
25. Porporato PE, Payen VL, Perez-Escuredo J, De Saedeleer CJ, Danhier P, Copetti T, et al. A mitochondrial switch promotes tumor metastasis. Cell Rep 2014;8:754–66.
26. Perez-Escuredo J, Dadhich RK, Dhup S, Cacace A, Van Hee VF, De Saedeleer CJ, et al. Lactate promotes glutamine uptake and metabolism in oxidative cancer cells. Cell Cycle 2016;15:72–83.
27. Van Hee VF, Labar D, Dehon G, Grasso D, Gregoire V, Muccioli GG, et al. Radiosynthesis and validation of (+/-)-[18F]-3-fluoro-2-hydroxypropionate ([18F]-FLac) as a PET tracer of lactate to monitor MCT1-dependent lactate uptake in tumors. Oncotarget 2017;8:24415–28.
28. Halestrap AP, Price NT. The proton-linked monocarboxylate transporter (MCT) family: structure, function and regulation. Biochem J 1999;343(Pt 2):281–99.
29. Halestrap AP. The SLC16 gene family - structure, role and regulation in health and disease. Mol Aspects Med 2013;34:337–49.
30. Van Hée VF, Perez-Escuredo J, Cacace A, Copetti T, Sonveaux P. Lactate does not activate NF-kB in oxidative tumor cells. Front Pharmacol 2015;6:228.
31. Tamura M, Gu J, Matsumoto K, Aota S, Parsons R, Yamada KM. Inhibition of cell migration, spreading, and focal adhesions by tumor suppressor PTEN. Science 1998;280:1614–7.
32. Gillet L, Roger S, Besson P, Lecaille F, Gore J, Bougnoux P, et al. Voltage-gated sodium channel activity promotes cysteine cathepsin-dependent invasiveness and colony growth of human cancer cells. J Biol Chem 2009;284:8680–91.
33. De Saedeleer CJ, Copetti T, Porporato PE, Verrax J, Feron O, Sonveaux P. Lactate activates HIF-1 in oxidative but not in Warburg-phenotype human tumor cells. PLoS One 2012;7:e46571.
34. Goetze K, Walenta S, Ksiazkiewicz M, Kunz-Schughart LA, Mueller-Klieser W. Lactate enhances motility of tumor cells and inhibits monocyte migration and cytokine release. Int J Oncol 2011;39:453–63.
35. Payen VL, Porporato PE, Baselet B, Sonveaux P. Metabolic changes associated with tumor metastasis, part 1: tumor pH, glycolysis and the pentose phosphate pathway. Cell Mol Life Sci 2016;73:1333–48.

36. Zhao Z, Wu MS, Zou C, Tang Q, Lu J, Liu D, et al. Downregulation of MCT1 inhibits tumor growth, metastasis and enhances chemotherapeutic efficacy in osteosarcoma through regulation of the NF-kappaB pathway. Cancer Lett 2014;342:150–8.
37. Burke JR, Pattoli MA, Gregor KR, Brassil PJ, MacMaster JF, McIntyre KW, et al. BMS-345541 is a highly selective inhibitor of I kappa B kinase that binds at an allosteric site of the enzyme and blocks NF-kappa B-dependent transcription in mice. J Biol Chem 2003;278:1450–6.
38. Cairns RA, Hill RP. A fluorescent orthotopic model of metastatic cervical carcinoma. Clin Exp Metastasis 2004;21:275–81.
39. Aslakson CJ, Miller FR. Selective events in the metastatic process defined by analysis of the sequential dissemination of subpopulations of a mouse mammary tumor. Cancer Res 1992;52:1399–405.
40. Carpenter L, Halestrap AP. The kinetics, substrate and inhibitor specificity of the lactate transporter of Ehrlich-Lettre tumour cells studied with the intracellular pH indicator BCECF. Biochem J 1994;304(Pt 3):751–60.
41. Froberg MK, Gerhart DZ, Enerson BE, Manivel C, Guzman-Paz M, Seacotte N, et al. Expression of monocarboxylate transporter MCT1 in normal and neoplastic human CNS tissues. Neuroreport 2001;12:761–5.
42. Lee GH, Kim DS, Chung MJ, Chae SW, Kim HR, Chae HJ. Lysyl oxidase-like-1 enhances lung metastasis when lactate accumulation and monocarboxylate transporter expression are involved. Oncol Lett 2011;2:831–8.
43. Gatenby RA, Gawlinski ET, Gmitro AF, Kaylor B, Gillies RJ. Acid-mediated tumor invasion: a multidisciplinary study. Cancer Res 2006; 66:5216–23.
44. Newell K, Franchi A, Pouyssegur J, Tannock I. Studies with glycolysis-deficient cells suggest that production of lactic acid is not the only cause of tumor acidity. Proc Natl Acad Sci U S A 1993;90:1127–31.
45. Becker HM, Hirnet D, Fecher-Trost C, Sultemeyer D, Deitmer JW. Transport activity of MCT1 expressed in Xenopus oocytes is increased by interaction with carbonic anhydrase. J Biol Chem 2005;280:39882–9.
46. Slomiany MG, Grass GD, Robertson AD, Yang XY, Maria BL, Beeson C, et al. Hyaluronan, CD44, and emmprin regulate lactate efflux and membrane localization of monocarboxylate transporters in human breast carcinoma cells. Cancer Res 2009;69:1293–301.
47. Noor SI, Dietz S, Heidtmann H, Boone CD, McKenna R, Deitmer JW, et al. Analysis of the binding moiety mediating the interaction between monocarboxylate transporters and carbonic anhydrase II. J Biol Chem 2015; 290:4476–86.
48. Kennedy KM, Dewhirst MW. Tumor metabolism of lactate: the influence and therapeutic potential for MCT and CD147 regulation. Future Oncol 2010;6:127–48.
49. Venkatesan B, Valente AJ, Prabhu SD, Shanmugam P, Delafontaine P, Chandrasekar B. EMMPRIN activates multiple transcription factors in cardiomyocytes, and induces interleukin-18 expression via Rac1-dependent PI3K/Akt/IKK/NF-kappaB andMKK7/JNK/AP-1 signaling. J Mol Cell Cardiol 2010;49:655–63.
50. Zhai Y, Wu B, Li J, Yao XY, Zhu P, Chen ZN. CD147 promotes IKK/IkappaB/NF-kappaB pathway to resist TNF-induced apoptosis in rheumatoid arthritis synovial fibroblasts. J Mol Med (Berl) 2016;94:71–82.